

Published in final edited form as:

*Nat Geosci.* 2019 October ; 12(10): 863–868. doi:10.1038/s41561-019-0443-2.

## Burma Terrane part of the Trans-Tethyan Arc during collision with India according to palaeomagnetic data

Jan Westerweel<sup>1,\*</sup>, Pierrick Roperch<sup>1</sup>, Alexis Licht<sup>2</sup>, Guillaume Dupont-Nivet<sup>1,3</sup>, Zaw Win<sup>4</sup>, Fernando Poblete<sup>1,5</sup>, Gilles Ruffet<sup>1</sup>, Hnin Hnin Swe<sup>6</sup>, Myat Kai Thi<sup>6</sup>, Day Wa Aung<sup>6</sup>

<sup>1</sup>Geosciences Rennes, CNRS, University of Rennes 1, Rennes, France

<sup>2</sup>Dept. Earth and Space Sciences, University of Washington, Seattle, United States

<sup>3</sup>Department of Earth Sciences, Potsdam University, Potsdam, Germany

<sup>4</sup>Department of Geology, University of Shwebo, Shwebo, Myanmar

<sup>5</sup>Instituto de Ciencias de la Ingeniería, Universidad de O'Higgins, Rancagua, Chile

<sup>6</sup>Department of Geology, University of Yangon, Yangon, Myanmar

### Abstract

Convergence between the Indian and Asian plates has reshaped large parts of Asia, changing regional climate and biodiversity. Yet geodynamic models fundamentally diverge on how convergence was accommodated since the India-Asia collision. Here we report paleomagnetic data from the Burma Terrane, at the eastern edge of the collision zone and famous for its Cretaceous amber biota, to better determine the evolution of the India-Asia collision. The Burma Terrane was part of a Trans-Tethyan island arc and stood at a near-equatorial southern latitude at ~95 Ma, suggesting island endemism for the Burmese amber biota. The Burma Terrane underwent significant clockwise rotation between ~80-50 Ma, causing its subduction margin to become hyper-oblique. Subsequently, it was translated northward on the Indian Plate, by an exceptional distance of at least 2000 km, along a dextral strike-slip fault system in the east. Our reconstructions are only compatible with geodynamic models involving a first collision of India with a near-equatorial Trans-Tethyan subduction system at ~60 Ma, followed by a later collision with the Asian margin.

---

The Himalayan-Tibetan orogen, resulting from terrane amalgamation including the India-Asia collision, is commonly considered as a natural laboratory for continent-continent collisional systems. Yet the paleogeography of the India-Asia collision remains a

---

Users may view, print, copy, and download text and data-mine the content in such documents, for the purposes of academic research, subject always to the full Conditions of use:[http://www.nature.com/authors/editorial\\_policies/license.html#terms](http://www.nature.com/authors/editorial_policies/license.html#terms)

\*Corresponding author: (jan.westerweel@univ-rennes1.fr).

#### Author contributions

P.R., A.L. and G.D.-N conceived the project. J.W., P.R., A.L., G.D.-N., Z.W., F.P., H.H.S., M.K.T. and D.W.A. participated in the sampling. J.W. and P.R. performed the paleomagnetic analysis. G.R. performed the radiometric analysis. J.W., P.R. and F.B. built the GPlates model. J.W., P.R., A.L. and G.D.-N. wrote the manuscript with contributions from other authors.

#### Competing interests

The authors declare no competing financial interests.

controversial issue <sup>1-5</sup> with widely different competing geodynamic models. For decades, a simple model prevailed proposing that the Indian plate moved northward until collision of Greater India with the Asian margin in the Eocene <sup>1,6</sup>. However, updated information supporting a Paleocene (~58 Ma <sup>7</sup>) collision age, alongside tectonic constraints, put the Indian continent at near-equatorial latitude at that time, thousands of kilometers away from the southern Asian margin <sup>3-6,8-13</sup>. A Paleocene collision could still be compatible with this first model by assuming an Asian margin at low latitude (~10°N <sup>6</sup>), but this is invalidated by paleomagnetic data <sup>14</sup>. Alternatively, an extra-large continental Greater India <sup>4</sup> could explain a Paleocene collision age. However, this would require unrealistic continental subduction of India <sup>4</sup> and major shortening of the Asian margin, which can only be partly solved by lateral extrusion of Indochina blocks away from the collision zone <sup>3,6,9-11</sup>, but remains much higher than accounted for by structural data <sup>15</sup>. Two new models have recently been proposed assuming: (1) the existence of an oceanic basin between India and Greater India that could have easily subducted after a first collision of Greater India with Asia at 58 Ma until a second collision of India with Asia in the Miocene <sup>5,12</sup>, or (2) the existence of a Trans-Tethyan subduction system with which the Indian continent would firstly collide at ~60-50 Ma, before jointly colliding with Asia later in the Paleogene <sup>2,16,17,8,13</sup>. Such a double subduction zone may also better account for the rapid India-Asia convergence prior to the final collision <sup>8</sup>.

The paleogeographic evolution of the Burma Terrane (BT, also named West Burma Block), at the eastern edge of the collision zone, is different in these geodynamic scenarios and therefore offers a way to determine the most realistic model (Fig. 1). For continental Greater India models <sup>3,6,9,10</sup>, the BT is located at a relatively high latitude during the Paleogene, next to the Lhasa Terrane as part of a linear ~E-W oriented Asian margin. From this position, the BT is extruded towards its present-day location. Because the volcanic arc of the BT, the Wuntho-Popa Arc, was interpreted as the eastward continuation of the Gangdese magmatic arc required in these models, but is nowadays ~N-S oriented (Fig. 2), these models necessitate significant post-collisional clockwise rotation for the BT. In the oceanic Greater India models <sup>12,5</sup>, the Asian margin is less deformed during the collision and the BT experienced little post-collisional rotation. Finally, the position of the BT is less constrained in Trans-Tethyan subduction models. Most reconstructions involving double subduction show the BT north of Sumatra <sup>13,17</sup>, but it could have also been part of the Incertus Arc, the island arc of the Trans-Tethyan subduction system <sup>17</sup>. This would potentially allow a more southern latitude for the BT during early collisional times <sup>2,8,13,16,17</sup>.

Presently, the paleogeographic evolution of the BT is virtually undocumented, despite being of critical importance for biodiversity studies, as the fossil amber from the BT harbours one of the most diverse and largest known records of Cretaceous biota <sup>18,19</sup>. Furthermore, the paleogeography of the BT is important for paleoenvironmental studies investigating Asian monsoonal history <sup>20,21</sup>. This study aims to fill this gap and solve these controversies by providing necessary constraints on the motion of the BT using new paleomagnetic and <sup>40</sup>Ar/<sup>39</sup>Ar age data.

## Geology of the Burma Terrane

The present-day BT geodynamic setting is characterized by hyper-oblique subduction of the Indian plate below the Burmese margin in the west and by the large-scale active dextral strike-slip Sagaing Fault in the east, resulting in a northward transcurrent motion of the terrane<sup>22</sup>. The western boundary of the BT is delineated by either another strike-slip fault, the Kabaw Fault, or the Naga Hills–Kalemyo–Andaman Ophiolite (herein called the Western Belt Ophiolite) in the Indo-Burman Ranges (IBR)<sup>23–26</sup>. The IBR basement has been interpreted as a separate tectonic block, accreted to the BT in the Early Cretaceous<sup>27</sup> or Late Cretaceous - Paleogene<sup>16,26</sup>, or an accretionary-type setting without block collision<sup>21,28,29</sup>. East of the BT, there is a complex succession of metamorphic rocks called the Mogok-Mandalay-Mergui Belt (MMMB), forming the boundary of the BT with the Shan Plateau (Sibumasu Block), alongside the Sagaing Fault and the Jade Belt ophiolite<sup>26</sup>. Total dextral displacement along this fault system has been estimated to be between 400 and 1100 km<sup>30–32</sup>. Prior to the development of the Sagaing Fault, there is evidence for dextral deformation along the Shan Scarp, directly east of the Sagaing fault<sup>33,34</sup>, although the tectonic regime of Sibumasu was predominantly sinistral<sup>35</sup>. Another example of earlier dextral deformation is the late Oligocene West Andaman Fault to the south<sup>34</sup>.

The oldest exposed rocks of the BT are the low-grade metamorphic Triassic Shwedaung and Pane Chung Formations, as well as the higher-grade Kanpetlet Schist. Both a late Mesozoic Gondwanan<sup>36</sup> or Cathaysian<sup>37</sup> origin has been suggested for the Pane Chung Formation, based on detrital zircon U-Pb age data. The Burmese margin formed as an Andean-type setting during the Cretaceous, evidenced by Andean-type magmatic activity in the Wuntho-Popa Arc that today crops out in the middle of a wide belt of forearc/back-arc basins which developed contemporaneously: The Central Myanmar Basins (Fig. 2)<sup>21,27,38</sup>. Published U-Pb data indicate an early Late Cretaceous main phase of magmatism from 110–85 Ma, followed by a 70–40 Ma subordinate stage<sup>39,24,27,40</sup>. Our new 97–87 Ma <sup>40</sup>Ar/<sup>39</sup>Ar dates in the Kanza Chung Batholith, the main unit of the northern Wuntho-Popa Arc (Fig. 2, Supplementary Data 1), confirm this major magmatic phase. The Western Belt Ophiolite was likely emplaced during that time as well<sup>21,27,28,38,41</sup>. The Wuntho-Popa Arc has been correlated with the similar Gangdese Arc (Lhasa Terrane)<sup>24,27</sup>. The correlation of the Gangdese arc with the Wuntho-Popa arc, and the correlation of the Western Belt Ophiolite with the Tibetan Yarlung-Tsangpo Suture Zone<sup>24,25</sup>, are key arguments for a similar to present-day latitude of the BT and a position next to the Lhasa Terrane prior to the India-Asia collision. However, the Mawgyi Andesite, which is most likely part of the Wuntho-Popa Arc (See Supplementary Information), has been correlated with the intra-oceanic mid-Cretaceous Woyla Arc (Sumatra)<sup>17,23,30</sup> as part of the Incertus Arc (Fig. 1)<sup>17</sup> with subsequent studies continuing this arc farther west by incorporating the Kohistan Arc (Pakistan)<sup>8,13</sup>.

## Paleomagnetic study

A paleomagnetic pole was obtained from a homoclinal sedimentary sequence in the upper Eocene (~38 Ma – from a dated tuff layer<sup>21</sup>) shallow-marine Yaw Formation in the Chindwin Basin, the northernmost forearc basin of Myanmar (Fig. 2). Furthermore, an early

Late Cretaceous pole was obtained from five localities (Pinlebu, Shinpa, Banmauk, Kawlin and Kyaung Le) in the Wuntho Range, the predominantly Cretaceous (~110-85 Ma<sup>24,40</sup>) northern segment of the Wuntho-Popa Arc, where the volcano-sedimentary rocks of the Kondan Chaung Group are intruded by I-type intrusions (Kanza Chaung Batholith) and andesitic stocks (Mawgyi Andesite). Detailed information on the geology, paleomagnetic analysis and <sup>40</sup>Ar/<sup>39</sup>Ar dating is provided in the Methods, Supplementary Information and Supplementary Data tables.

The upper Eocene samples are from mudstones and siderite beds with primary detrital or early-diagenetic magnetizations, mostly carried by magnetite. They yield well-defined antipodal normal and reverse polarity directions in coherent magnetozones, resulting in a mean with a north oriented declination and shallow positive inclination in tectonic coordinates (Fig. 3a, Supplementary Data 1). This corresponds to a negligible rotation ( $4.6 \pm 3.5^\circ$ ) compared to stable Eurasia<sup>42</sup> and a near-equatorial latitude of  $2.4 \pm 1.5^\circ\text{N}$ . A slightly higher, but not significantly different  $4.1 \pm 2.3^\circ\text{N}$  paleolatitude is obtained after inclination shallowing corrections (See Supplementary Information). This result is corroborated by similarly low inclinations obtained from the siderite beds devoid of shallowing, and in general agreement with the low impact of inclination shallowing in sedimentary rocks at low latitudes, compared to mid to high latitudes<sup>43</sup>.

In early Late Cretaceous rocks from the Wuntho Range, reliable directions were obtained from sites of the Kanza Chaung Batholith (Pinlebu, Shinpa and Banmauk) with characteristic remanent magnetizations (ChRMs) carried by magnetite, as well as sites from the Kondan Chaung Group (Kawlin, Kyaung Le), which were homogeneously magnetized during emplacement of the batholith, as shown by our petrologic observations and <sup>40</sup>Ar/<sup>39</sup>Ar dates (See Supplementary Information). Blocking temperatures of the ChRMs are similar to the closure temperatures in <sup>40</sup>Ar/<sup>39</sup>Ar dating, suggesting the age of magnetization of the Wuntho rocks to be around ~97-87 Ma, in accordance with existing Wuntho-Popa Arc U-Pb data<sup>24,40</sup>. A systematic trend to east-directed declinations and horizontal to slightly negative inclinations can be inferred from our data (Supplementary Data 1), despite significant differences in rock types and magnetic properties. Tilting is recorded by rocks of the Kondan Chaung Group, but occurred prior to the intrusion of the batholith in most cases. No field evidence for significant tilting of the Kanza Chaung Batholith was observed, in agreement with our anisotropy of magnetic susceptibility (AMS) data (See Supplementary Information). If we omit data from brecciated and non-homogeneously hydrothermally altered sites from the Mawgyi Andesite (Kawlin), and the westernmost sites from the Kondan Chaung Group (Kyaung Le), which were slightly tilted after acquiring their magnetization, we obtain a similar, but better defined overall final mean direction for the Wuntho Range from 16 sites (Fig. 3b, Supplementary Data 1). The mean corresponds to a slightly southern hemisphere paleolatitude of  $5.0 \pm 4.7^\circ\text{S}$  for the BT in the early Late Cretaceous and a significant clockwise rotation ( $60.4 \pm 8.7^\circ$ ) with respect to the expected direction from stable Eurasia<sup>42</sup>. This implies that most rotation of the BT occurred between the early Late Cretaceous and late Eocene with ~800 km of northward motion (Fig. 3c). Although we cannot discard a component of local rotation associated with dextral shear, the systematic rotation values and the regionally-coherent N-S trends of the batholith and main tectonic structures, suggest that the mean declination better reflects a wholesale rotation of

the Wuntho rocks. The near-equatorial early Late Cretaceous – late Eocene paleolatitudes implied by our data are in stark contrast with previous studies, usually placing the BT close to its present-day location since the early Cenozoic, <sup>17,24,34,26,27</sup> and these data therefore have major tectonic implications.

## Tectonic implications

The southern hemisphere shallow latitude at ~95 Ma for the Wuntho Arc is distant from the southern Asian margin and Indochina and is therefore best explained as having been formed above a near-equatorial Trans-Tethyan subduction system, as part of the Incertus Arc, with northward subducting Neo-Tethyan oceanic lithosphere (Fig. 4) <sup>8</sup>. This is further supported by the development of the Burmese margin as an Andean-type setting around that time (Late Cretaceous) and coeval emplacement of the Western Belt Ophiolite <sup>21,24,27,28,38,40,41</sup>. The Trans-Tethyan subduction system could have been partly intra-oceanic, possibly incorporating the Kohistan Arc which also formed at near-equatorial latitude <sup>8,44</sup>. Because the Indonesian Woyla Arc is interpreted as being already accreted at ~90 Ma <sup>17,23</sup>, we reconstructed a transform fault east of the BT, accommodating an earlier Woyla Arc - Sundaland collision.

The major clockwise rotation of the BT between 95 and 40 Ma (Fig. 4) may be either linked to the accretion of the BT to the margin of southern Sibumasu/northern Sundaland or the collision of India with the Trans-Tethyan subduction system. In support of the latter possibility is that in most models with Trans-Tethyan subduction <sup>8,13,16</sup>, decreasing convergence rates between India and Asia at ~60-50 Ma are associated with collision of the (Greater) Indian continent with the arc. At the eastern end of this collision, thin Indian continental crust may thus have interacted with the BT, causing its clockwise rotation <sup>45</sup>. However, the exact timing and mechanism of this rotation needs to be refined with future research.

Since the late Eocene (~38 Ma <sup>21</sup>), our results indicate a significant ~2000 km northward motion, coeval with the motion of India (Fig. 4), during a period when Indochina is extruded towards the south-east <sup>46-49</sup>. This suggests that the northward motion of the BT was coupled with the Indian Plate. Our paleomagnetic data indicate that the Burmese subduction margin was already oriented approximately N-S in the late Eocene, such that subduction of the Indian Plate beneath the BT was already hyper-oblique. This hyper-obliquity provides a mechanism for the full-partitioning of the Burmese subduction margin relative to Indochina and its coupling with the Indian motion; it is also consistent with the inferred onset of pull-apart subsidence in the Chindwin Basin <sup>21</sup> and a significant decrease in Wuntho-Popa Arc magmatism at ~38 Ma <sup>27,40</sup>. Furthermore, the coeval motion of the BT and India suggests that dextral wrenching within the IBR has not been important until the Neogene.

Hence, the northward motion of the BT since the late Eocene requires a major dextral strike-slip system east of the BT. However, the ~2000 km northward motion indicated by our paleomagnetic data is much more than the ~400 km of motion estimated along the active dextral Sagaing Fault at the eastern margin of the BT <sup>31</sup>. Furthermore, the age of the Sagaing Fault - Quaternary, Neogene, or older - remains debated <sup>30-32</sup>. A precursor dextral strike-slip

system is thus required by our data, pathway and location of which remains enigmatic and has probably been obscured by posterior activity of the Sagaing Fault and opening of the Andaman Sea. Potential remnants of this precursor strike-slip system are an early segment of the Sagaing Fault<sup>33,34</sup> or the Oligocene West Andaman Fault<sup>34</sup>. The latter could have effectively separated the BT to its west from the developing Eastern Andaman Basins and the predominantly sinistral tectonic regime of Sibumasu to its east, as the BT moved northward and passed west of these features (Fig. 4)<sup>32,34,35</sup>. This separation potentially explains why late Eocene sedimentary infill of the Central Myanmar Basins was predominantly derived from an Andean-type arc, likely the Wuntho-Popa Arc, with an increasing contribution of older metamorphic detritus in the Oligocene – Miocene<sup>21</sup> as the BT moved closer to Sibumasu and the eastern Himalayan syntaxis.

Additionally, the late Eocene low paleolatitude for the BT demonstrates that an India-BT collision next to the Lhasa Terrane<sup>2</sup> is impossible. Instead, the near-equatorial latitude of the BT provides the space and free border for the lateral extrusion of the Tengshong and Baoshan Blocks which rotated clockwise by ~40-70°<sup>47,48</sup> and, to a minor extent, the Indochina Block that rotated ~15-20°, all of which occurred mainly during the Oligocene – Miocene. This is the period of major sinistral deformation along the main shear zones separating these blocks<sup>46,49</sup>. The northward motion and later emplacement without rotation of the BT also accounts for the striking difference between the linear N-S orientation of the Sagaing Fault and - directly to the west- the curvilinear sinistral faults (Gaoligong, Wanding, Nanting) associated with the clockwise rotations in the Tengshong and Baoshan Blocks.

Beyond geodynamics, our results suggest that the BT was isolated as part of the Incertus Arc at the time of deposition of the prolific Cretaceous Burmese fossil ambers, which raises questions about the potential endemic character of the amber biota and their connection with species from India, Gondwana and SE Asia<sup>18,19</sup>. From a paleoenvironmental perspective, our near-equatorial paleolatitudes for the BT are surprising, considering the evidence for strongly seasonal climate in Myanmar in the Eocene<sup>20</sup>. Strong seasonality at Eocene equatorial latitudes in SE Asia is corroborated by independent evidence from paleoclimatic data from Java<sup>50</sup>. Paleomagnetic and paleoenvironmental data can only be reconciled with a massive seasonal migration of the Intertropical Convergence Zone over SE Asia, confirming well-marked South Asian monsoons during the Eocene<sup>20</sup>, although future climate models incorporating our new reconstructions need to verify this.

The foremost conclusion from our paleomagnetic results is that they are incompatible with both continental and oceanic Greater India models and are best interpreted in a geodynamic framework with a Trans-Tethyan subduction system accommodating India-Asia convergence. As part of this system, the BT was a segment of the Incertus Arc, when Neo-Tethyan subduction started in the Late Cretaceous. In the period including the early Paleogene collision of India with the Trans-Tethyan subduction system, the BT rotated ~60° clockwise, and then moved northward at least 2000 km since ~38 Ma, as part of the Indian Plate, along a dextral strike-slip system until it reached its present-day position. Hence, our findings provide much needed evidence to settle a longstanding geodynamic debate on the India-Asia collision and the existence of a Trans-Tethyan subduction system. Furthermore, they pave the way to reinterpreting regional structural and paleogeographic data by taking

into account the near-equatorial position for the BT during the Late Cretaceous to Eocene as part of this system.

## Methods

### Paleomagnetic sampling

Conventional paleomagnetic core plug samples were obtained from two localities in northern Myanmar, both part of the Burma Terrane (BT). Sampling and orientation of the samples were done using standard paleomagnetic field equipment and procedures with both magnetic and sun compasses. The first locality consists of the early Late Cretaceous intrusive, extrusive, volcanoclastic and sedimentary rocks of the Wuntho Range, near the towns of Kawlin, Pinlebu, Shinpa, Banmauk and Kyaung Le, and the second locality of upper Eocene sedimentary rocks in the Chindwin forearc basin, near the town of Kalewa. A detailed geologic setting, including regional maps, is provided in the Supplementary Information.

We sampled 19 sites in intrusive rocks, 13 sites in extrusive rocks and 9 sites in sedimentary rocks of early Late Cretaceous age in the Wuntho Range, mostly drilled in recently exposed quarries or rivers, providing fresh samples with almost no weathering. Most sites in intrusive rocks were drilled around Pinlebu, Shinpa and Banmauk in the western and northern part of the study area. These sites belong to the regional I-type Kanza Chaung Batholith, which constitutes the main component of the Wuntho Range. Near Kawlin in the southern part of the study area, 11 sites in extrusive rocks of the Mawgyi Andesite Formation were established. The volcanic rocks are often massive or brecciated; hence they did not yield clear bedding orientations. Apart from these sites in andesites, two sites in sandstones from the volcano-sedimentary Kondan Chaung Group with a clearly observable bedding and one undefined stock were sampled near Kawlin. At Kyaung Le in the northernmost part of the study area, all sampled rocks belong to the Kondan Chaung Group, and consist of nine sites in sedimentary and volcanoclastic rocks, as well as one rhyodacitic unit and finally one site in undefined extrusive rocks.

In the Chindwin basin, 520 samples were collected from the upper Eocene shallow-marine Yaw Formation in a continuous homoclinal Cenozoic sedimentary section near Kalewa, as well as two additional sites. Most of these samples are mudstones and sandstones, and we also collected several samples in siderite-rich carbonate beds intercalated in the mudstones.

### Paleomagnetic analysis

Natural Remanent Magnetizations (NRM) were measured on a 2G cryogenic magnetometer hosted in a magnetically shielded room at the University of Rennes 1. Stepwise demagnetization was used to isolate their Characteristic Remanent Magnetization (ChRM) components, using either thermal demagnetization, with increments of 20-50°C up to 680°C, or 3-axis Alternating Field (AF) demagnetization, with increments of 2.5-10 mT up to 120 mT. During the AF demagnetization, Gyro Remanent Magnetizations (GRMs) were cancelled by measuring the magnetization after each axis of AF demagnetization<sup>51</sup>. Samples with interpretable components were grouped per site after isolating their ChRM

using principal component analysis<sup>52</sup>, and when necessary a great-circle approach<sup>53</sup>. Subsequently, mean directions and corresponding statistical parameters were calculated per site and finally per locality using Fisher statistics<sup>54,55</sup>. Whenever possible, the fold test<sup>56</sup> was utilized to investigate whether the magnetization was pre- or post-tectonic in origin. To check whether normal and reverse polarities from the same locality are antiparallel, the classic coordinate bootstrap reversal test was used<sup>57</sup>. Finally, due to the lack of volcanic rocks in the upper Eocene sedimentary section, we checked for inclination shallowing in the results from this area, using several approaches including the classic Elongation versus Inclination (E/I) method<sup>58–60</sup>, and by assuming that the sedimentary package consists of uniform rigid particles, which rotate during burial and attending compaction<sup>61</sup>.

In addition to obtaining mean directions, the magnetic properties of the samples were investigated using several methods. After each thermal demagnetization step, the bulk magnetic susceptibility of the samples was measured. To investigate the mineralogy and magnetic properties for a selection of samples, we measured mass-normalized bulk magnetic susceptibility curves with increasing temperature steps up to 580 °C on a KLY3-CS3 AGICO kappabridge, as well as magnetic hysteresis loops on a MicroMag vibrating sample magnetometer. To further identify the possible effect of a magnetic fabric on the remanent magnetization for the different rocks, anisotropy of magnetic susceptibility (AMS) was determined for most samples on a KLY3S AGICO kappabridge. In highly anisotropic intrusive igneous rocks, Thermal Remanent Magnetization (TRM) vectors may be deflected from the direction of the field upon cooling below the Curie point of magnetite, which is the main magnetic carrier in those rocks. However, most of the AMS is likely dictated by multidomain magnetite, yet the magnetic carriers of the remanent magnetization (finest grained magnetite) may have a different magnetic fabric. For this reason, we investigated the anisotropy of remanent magnetization (ARM) in selected samples of intrusive rocks. TRM anisotropy correction is common in archeomagnetism, but we did not attempt this, because it requires heating of the samples above 580°C (general NRM unblocking temperature), and alteration is likely to occur after heating to higher temperatures. Anisotropy of isothermal remanent magnetization (IRM) was performed on selected samples instead. IRM acquisition was done on x,-x,y,-y,z,-z at 600 mT, well above the saturation field of magnetite (250 mT). After each measurement, the sample was AF demagnetized at 20 mT to remove the lowest magnetic coercivity fraction. In most cases, 90% of the full IRM was randomized at 20 mT.

A detailed description of the various ChRM characteristics, mean calculations, tests and magnetic properties is given per locality in the Supplementary Information. The paleomagnetic results per site and per locality is given in Supplementary Data 1, while the results all used samples are listed in Supplementary Data 2.

## Petrology

Polished thin sections were made on selected samples from different lithologies for observation under an optical microscope in transmitted light and reflected light. The samples were then analysed with a scanning electron microscope (SEM - JEOL JSM 7100F with energy dispersive X-ray spectroscopy - Oxford EDS/EBSD) at the CMEBA - ScanMAT

platform (University of Rennes 1). Our petrologic observations are described in the Supplementary Information.

### **$^{40}\text{Ar}/^{39}\text{Ar}$ dating**

There are only a few available U-Pb age data available for the Wuntho Range volcanic complex <sup>24,39</sup>. Therefore, we carried out  $^{40}\text{Ar}/^{39}\text{Ar}$  dating on 14 samples from our paleomagnetic sites in order to better understand the ages of these rocks and their resulting ChRMs.

Samples were analysed with an  $^{40}\text{Ar}/^{39}\text{Ar}$  laser probe and a Map 215 mass spectrometer. Analyses were performed on mm-sized grains of single biotite or amphibole crystals, carefully handpicked under a binocular microscope from crushed rocks. For samples with fine-grained matrix from which it was not possible to extract biotites or amphiboles, experiments were performed on whole-rock samples.

Irradiation of samples was performed at McMaster Nuclear Reactor (Hamilton, Ontario, Canada) in the 8F facility and lasted 66.667 h with a global efficiency (J/h) of  $9.767 \times 10^{-5}\text{h}^{-1}$ . The irradiation standard was sanidine TCRs ( $28.608 \pm 0.033 \text{ Ma}$  <sup>62-64</sup>).

Apparent age errors are plotted at the  $1\sigma$  level and do not include the errors on the  $^{40}\text{Ar}^*/^{39}\text{Ar}_K$  ratio and age of the monitor and decay constant. Plateau ages were calculated if 70% or more of the  $^{39}\text{Ar}_K$  was released in at least three or more contiguous steps, the apparent ages of which agreeing to within  $1\sigma$  of the integrated age of the plateau segment. Pseudo-plateau ages can be defined with less than 70% of the  $^{39}\text{Ar}_K$  released and possibly less than three contiguous steps. The errors on the  $^{40}\text{Ar}^*/^{39}\text{Ar}_K$  ratio and age of the monitor and decay constant are included in the final calculation of the error margins on the (pseudo-)plateau ages.

Analytical data and parameters used for calculations (e.g. isotopic ratios measured on K, Ca and Cl pure salts; mass discrimination; atmospheric argon ratios; J parameter; decay constants) and reference sources are available in Supplementary Data 3.

### **Plate model**

For our final geodynamic model, we used the global rotations and continental polygons from the Matthews 2016 GPlates model <sup>65,66</sup> as a template. From this template, we modified the tectonic history of the BT to reflect our paleomagnetic results. Furthermore, the positions and paleogeography of Greater India, Indochina, Kohistan, Lhasa, Sumatra and Woyla were configured to better reflect more recent studies <sup>8,67,68</sup>. In Figure 1b, the global reconstruction with the Greater India basin hypothesis is based on a different set of poles of rotations <sup>5</sup>. All plate tectonic reconstructions were made in the combined hotspot (0-70 Ma) and paleomagnetic (70-250 Ma) reference frame that is also used in the Matthews 2016 GPlates model <sup>66,69</sup>. See Supplementary Information for a detailed discussion on the choice for this reference frame.

## Supplementary Material

Refer to Web version on PubMed Central for supplementary material.

## Acknowledgements

This research was primarily funded by the ERC consolidator grant MAGIC 649081 to G.D.-N.. We thank Catherine Kissel for the use of the AGM vibrating magnetometer at the LSCE paleomagnetic laboratory, France. Furthermore, we thank Loic Joanny and Francis Gouttefangeas for their help with SEM data acquisition. We are grateful to P. Cullerier and A. Bernard for their help in the laboratory. We thank Eldert Advokaat, Frédéric Fluteau, Stéphane Guillot, Erwan Hallot, Claude Rangin, Anne Replumaz, Mike Searle and Douwe van Hinsbergen for prolific discussions in the course of this study. Finally, we are grateful to Chris Morley, Robert Hall and John Geissman for their constructive reviews, which helped to clarify our data presentation and model.

## Data availability

The authors declare that all data supporting the findings of this study are available within the main article, its Supplementary Information, Supplementary Data 1 (paleomagnetic mean directions), Supplementary Data 2 (paleomagnetic data per sample) and Supplementary Data 3 ( $^{40}\text{Ar}/^{39}\text{Ar}$  data and parameters).

## References

1. Molnar P, Tapponnier P. Cenozoic Tectonics of Asia: Effects of a Continental Collision: Features of recent continental tectonics in Asia can be interpreted as results of the India-Eurasia collision. *Science*. 1975; 189:419–426. [PubMed: 17781869]
2. Aitchison JC, Ali JR, Davis AM. When and where did India and Asia collide? *J Geophys Res*. 2007; 112
3. Replumaz A, Negredo AM, Guillot S, Villaseñor A. Multiple episodes of continental subduction during India/Asia convergence: Insight from seismic tomography and tectonic reconstruction. *Tectonophysics*. 2010; 483:125–134.
4. Ingalls M, Rowley DB, Currie B, Colman AS. Large-scale subduction of continental crust implied by India–Asia mass-balance calculation. *Nat Geosci*. 2016; 9:848–853.
5. van Hinsbergen DJJ, et al. Reconstructing Greater India: Paleogeographic, kinematic, and geodynamic perspectives. *Tectonophysics*. 2018; doi: 10.1016/j.tecto.2018.04.006
6. Cogne J-P, Besse J, Chen Y, Hankard F. A new Late Cretaceous to Present APWP for Asia and its implications for paleomagnetic shallow inclinations in Central Asia and Cenozoic Eurasian plate deformation. *Geophys J Int*. 2013; 192:1000–1024.
7. Hu X, et al. The timing of India-Asia collision onset – Facts, theories, controversies. *Earth-Sci Rev*. 2016; 160:264–299.
8. Jagoutz O, Royden L, Holt AF, Becker TW. Anomalously fast convergence of India and Eurasia caused by double subduction. *Nat Geosci*. 2015; 8:475–478.
9. Replumaz A, Guillot S, Villaseñor A, Negredo AM. Amount of Asian lithospheric mantle subducted during the India/Asia collision. *Gondwana Res*. 2013; 24:936–945.
10. Royden LH, Burchfiel BC, van der Hilst RD. The Geological Evolution of the Tibetan Plateau. *Science*. 2008; 321:1054–1058. [PubMed: 18719275]
11. Tapponnier P, Peltzer G, Le Dain AY, Armijo R, Cobbold P. Propagating extrusion tectonics in Asia: New insights from simple experiments with plasticine. *Geology*. 1982; 10:611–616.
12. Van Hinsbergen DJ, et al. Greater India Basin hypothesis and a two-stage Cenozoic collision between India and Asia. *Proc Natl Acad Sci*. 2012; 109:7659–7664. [PubMed: 22547792]
13. Zahirovic S, Seton M, Müller RD. The Cretaceous and Cenozoic tectonic evolution of Southeast Asia. *Solid Earth*. 2014; 5:227–273.

14. Dupont-Nivet G, Lippert PC, Van Hinsbergen DJJ, Meijers MJM, Kapp P. Palaeolatitude and age of the Indo-Asia collision: palaeomagnetic constraints: Palaeolatitude and age of the Indo-Asia collision. *Geophys J Int.* 2010; 182:1189–1198.
15. van Hinsbergen DJJ, et al. Restoration of Cenozoic deformation in Asia and the size of Greater India. *Tectonics.* 2011; 30
16. Gibbons AD, Zahirovic S, Müller RD, Whittaker JM, Yatheesh V. A tectonic model reconciling evidence for the collisions between India, Eurasia and intra-oceanic arcs of the central-eastern Tethys. *Gondwana Res.* 2015; 28:451–492.
17. Hall R. Late Jurassic–Cenozoic reconstructions of the Indonesian region and the Indian Ocean. *Tectonophysics.* 2012; 570–571:1–41.
18. Poinar G. Burmese amber: evidence of Gondwanan origin and Cretaceous dispersion. *Hist Biol.* 2018; :1–6. DOI: 10.1080/08912963.2018.1446531
19. Grimaldi DA, Engel MS, Nascimbene PC. Fossiliferous Cretaceous Amber from Myanmar (Burma): Its Rediscovery, Biotic Diversity, and Paleontological Significance. *Am Mus Novit.* 2002; 3361:1–71.
20. Licht A, et al. Asian monsoons in a late Eocene greenhouse world. *Nature.* 2014; 513:501–506. [PubMed: 25219854]
21. Licht A, et al. Paleogene evolution of the Burmese forearc basin and implications for the history of India-Asia convergence. *Geol Soc Am Bull.* 2018; 1:20.
22. Socquet A, et al. India and Sunda plates motion and deformation along their boundary in Myanmar determined by GPS. *J Geophys Res Solid Earth.* 2006; 111
23. Barber AJ, Crow MJ. Structure of Sumatra and its implications for the tectonic assembly of Southeast Asia and the destruction of Paleotethys. *Isl Arc.* 2009; 18:3–20.
24. Mitchell A, Chung S-L, Oo T, Lin T-H, Hung C-H. Zircon U–Pb ages in Myanmar: Magmatic–metamorphic events and the closure of a neo-Tethys ocean? *J Asian Earth Sci.* 2012; 56:1–23.
25. Liu C-Z, et al. Tethyan suturing in Southeast Asia: Zircon U-Pb and Hf-O isotopic constraints from Myanmar ophiolites. *Geology.* 2016; 44:311–314.
26. Searle MP, et al. Chapter 12 Tectonic and metamorphic evolution of the Mogok Metamorphic and Jade Mines belts and ophiolitic terranes of Burma (Myanmar). *Geol Soc Lond Mem.* 2017; 48:261–293.
27. Zhang P, et al. Structures, uplift, and magmatism of the Western Myanmar Arc: Constraints to mid-Cretaceous–Paleogene tectonic evolution of the western Myanmar continental margin. *Gondwana Res.* 2017; 52:18–38.
28. Fareeduddin A, Dilek Y. Structure and petrology of the Nagaland-Manipur Hill ophiolitic mélange zone NE India Foss Tethyan Subduction Channel India-Burma Plate Bound. *Episodes.* 2015; 38:298–314.
29. Zhang J, et al. Multiple alternating forearc- and backarc-ward migration of magmatism in the Indo-Myanmar Orogenic Belt since the Jurassic: Documentation of the orogenic architecture of eastern Neotethys in SE Asia. *Earth-Sci Rev.* 2018; 185:704–731.
30. Mitchell AHG. Cretaceous–Cenozoic tectonic events in the western Myanmar (Burma)–Assam region. *J Geol Soc.* 1993; 150:1089–1102.
31. Morley CK. Syn-kinematic sedimentation at a releasing splay in the northern Minwun Ranges, Sagaing Fault zone, Myanmar: significance for fault timing and displacement. *Basin Res.* 2017; 29:684–700.
32. Morley CK, Arboit F. Dating the onset of motion on the Sagaing fault: Evidence from detrital zircon and titanite U-Pb geochronology from the NorthMinwun Basin, Myanmar. *Geology.* 2019; doi: 10.1130/G46321.1
33. Bertrand G, Rangin C. Tectonics of the western margin of the Shan plateau (central Myanmar): implication for the India–Indochina oblique convergence since the Oligocene. *J Asian Earth Sci.* 2003; 21:1139–1157.
34. Morley CK. Chapter 4 Cenozoic rifting, passive margin development and strike-slip faulting in the Andaman Sea: a discussion of established v. new tectonic models. *Geol Soc Lond Mem.* 2017; 47:27–50.

35. Morley CK. Nested strike-slip duplexes, and other evidence for Late Cretaceous–Palaeogene transpressional tectonics before and during India–Eurasia collision, in Thailand, Myanmar and Malaysia. *J Geol Soc.* 2004; 161:799–812.
36. Yao W, et al. Origin and tectonic evolution of upper Triassic Turbidites in the Indo-Burman ranges, West Myanmar. *Tectonophysics.* 2017; 721:90–105.
37. Sevastjanova I, et al. Myanmar and Asia united, Australia left behind long ago. *Gondwana Res.* 2016; 32:24–40.
38. Pivnik DA, et al. Polyphase Deformation in a Fore-Arc/Back-Arc Basin, Salin Subbasin, Myanmar (Burma). *AAPG Bull.* 1998; 82(10):1837–1856.
39. Gardiner NJ, et al. Contrasting Granite Metallogeny through the Zircon Record: A Case Study from Myanmar. *Sci Rep.* 2017; 7
40. Wang J-G, Wu F-Y, Tan X-C, Liu C-Z. Magmatic evolution of the Western Myanmar Arc documented by U–Pb and Hf isotopes in detrital zircon. *Tectonophysics.* 2014; 612–613:97–105.
41. Singh AK, et al. Evidence of Mid-ocean ridge and shallow subduction forearc magmatism in the Nagaland-Manipur ophiolites, northeast India: constraints from mineralogy and geochemistry of gabbros and associated mafic dykes. *Geochemistry.* 2016; 76:605–620.
42. Torsvik TH, et al. Phanerozoic polar wander, palaeogeography and dynamics. *Earth-Sci Rev.* 2012; 114:325–368.
43. Arason P, Levi S. Models of inclination shallowing during sediment compaction. *J Geophys Res.* 1990; 95:4481.
44. Zaman H, Torii M. Palaeomagnetic study of Cretaceous red beds from the eastern Hindukush ranges, northern Pakistan: palaeoreconstruction of the Kohistan-Karakoram composite unit before the India-Asia collision. *Geophys J Int.* 1999; 136:719–738.
45. Rangin C, Maurin T, Masson F. Combined effects of Eurasia/Sunda oblique convergence and East-Tibetan crustal flow on the active tectonics of Burma. *J Asian Earth Sci.* 2013; 76:185–194.
46. Leloup PH, Tapponnier P, Lacassin R, Searle MP. Discussion on the role of the Red River shear zone, Yunnan and Vietnam, in the continental extrusion of SE Asia *Journal*, Vol. 163, 2006 1025–1036. *J Geol Soc.* 2007; 164:1253–1260.
47. Li S, van Hinsbergen DJJ, Deng C, Advokaat EL, Zhu R. Paleomagnetic Constraints From the Baoshan Area on the Deformation of the Qiangtang-Sibumasu Terrane Around the Eastern Himalayan Syntaxis. *J Geophys Res Solid Earth.* 2018; 123:977–997.
48. Tong Y-B, et al. Internal crustal deformation in the northern part of Shan-Thai Block: New evidence from paleomagnetic results of Cretaceous and Paleogene redbeds. *Tectonophysics.* 2013; 608:1138–1158.
49. Wang Y, et al. Kinematics and  $^{40}\text{Ar}/^{39}\text{Ar}$  geochronology of the Gaoligong and Chongshan shear systems, western Yunnan, China: Implications for early Oligocene tectonic extrusion of SE Asia. *Tectonophysics.* 2006; 418:235–254.
50. Evans D, Müller W, Oron S, Renema W. Eocene seasonality and seawater alkaline earth reconstruction using shallow-dwelling large benthic foraminifera. *Earth Planet Sci Lett.* 2013; 381:104–115.
51. Roperch P, Taylor GK. The importance of gyromagnetic remanence in alternating field demagnetization. Some new data and experiments on GRM and RRM. *Geophys J Int.* 1986; 87:949–965.
52. Kirschvink JL. The least-squares line and plane and the analysis of palaeomagnetic data. *Geophys J Int.* 1980; 62:699–718.
53. McFadden PL, McElhinny M. The combined analysis of remagnetisation circles and direct observation in palaeomagnetism. *Earth Planet Sci Lett.* 1988; 87:161–172.
54. Butler, RF. *Paleomagnetism: magnetic domains to geologic terranes.* Vol. 319. Blackwell Scientific Publications; Boston: 1992.
55. Fisher R. Dispersion on a sphere. *Proc R Soc Lond Ser Math Phys Sci.* 1953; 217:295–305.
56. Tauxe L, Watson GS. The fold test: an eigen analysis approach. *Earth Planet Sci Lett.* 1994; 122:331–341.
57. Tauxe, L. *Essentials of paleomagnetism.* Univ of California Press; 2010.

58. King RF. The remanent magnetism of artificially deposited sediments. *Geophys J Int.* 1955; 7:115–134.
59. Tauxe L, Kent DV. A simplified statistical model for the geomagnetic field and the detection of shallow bias in paleomagnetic inclinations: was the ancient magnetic field dipolar. *Timescales Paleomagn Field.* 2004; 145:101–116.
60. Tauxe L, Kodama KP, Kent DV. Testing corrections for paleomagnetic inclination error in sedimentary rocks: a comparative approach. *Phys Earth Planet Inter.* 2008; 169:152–165.
61. Cogné, J-P. Contribution a l'étude paléomagnétique des roches déformées. Vol. 1. Université Rennes; 1987.
62. Renne PR, et al. Intercalibration of standards, absolute ages and uncertainties in  $^{40}\text{Ar}/^{39}\text{Ar}$  dating. *Chem Geol.* 1998; 145:117–152.
63. Renne PR, Mundil R, Balco G, Min K, Ludwig KR. Joint determination of  $^{40}\text{K}$  decay constants and  $^{40}\text{Ar}^*/^{40}\text{K}$  for the Fish Canyon sanidine standard, and improved accuracy for  $^{40}\text{Ar}/^{39}\text{Ar}$  geochronology. *Geochim Cosmochim Acta.* 2010; 74:5349–5367.
64. Renne PR, Balco G, Ludwig KR, Mundil R, Min K. Response to the comment by W.H. Schwarz et al. on “Joint determination of  $^{40}\text{K}$  decay constants and  $^{40}\text{Ar}^*/^{40}\text{K}$  for the Fish Canyon sanidine standard, and improved accuracy for  $^{40}\text{Ar}/^{39}\text{Ar}$  geochronology” by P.R. Renne et al. (2010). *Geochim Cosmochim Acta.* 2011; 75:5097–5100.
65. Müller RD, et al. GPlates: Building a virtual Earth through deep time. *Geochem Geophys Geosystems.* 2018; 19:2243–2261.
66. Matthews KJ, et al. Global plate boundary evolution and kinematics since the late Paleozoic. *Glob Planet Change.* 2016; 146:226–250.
67. Advokaat EL, et al. Cenozoic Rotation History of Borneo and Sundaland, SE Asia Revealed by Paleomagnetism, Seismic Tomography, and Kinematic Reconstruction. *Tectonics.* 2018; doi: 10.1029/2018TC005010
68. Li S, et al. Paleomagnetic constraints on the Mesozoic–Cenozoic paleolatitudinal and rotational history of Indochina and South China: Review and updated kinematic reconstruction. *Earth-Sci Rev.* 2017; 171:58–77.
69. Torsvik TH, Müller RD, Van der Voo R, Steinberger B, Gaina C. Global plate motion frames: Toward a unified model. *Rev Geophys.* 2008; 46

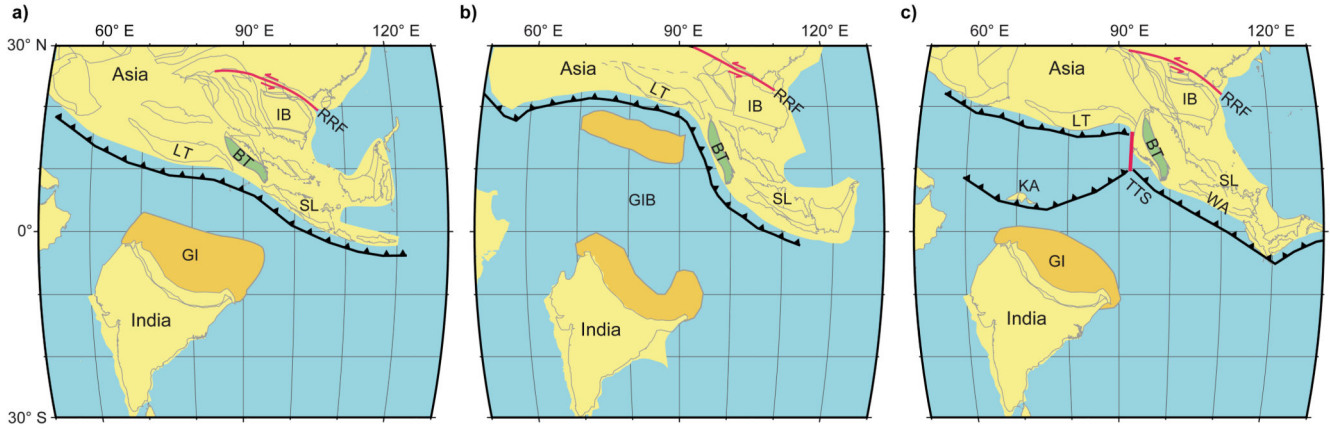


**Figure 1.**

Alternative plate reconstructions of India-Asia paleogeography at 60 Ma with GPlates (See also Methods): a) Reconstruction with a nearly linear subduction zone and significant extrusion of Indochina blocks<sup>6,9</sup>; b) Reconstruction with a Greater India Basin<sup>5</sup>; c) Reconstruction with a second Trans-Tethyan subduction zone<sup>13</sup>. Abbreviations: BT = Burma Terrane, GI(B) = Greater India (Basin), IB = Indochina Blocks, KA = Kohistan Arc, LT = Lhasa Terrane, RRF = Red River Fault (accommodating Indochina extrusion), SL = Sundaland, TTS = Trans-Tethyan subduction system, WA = Woyla Arc.

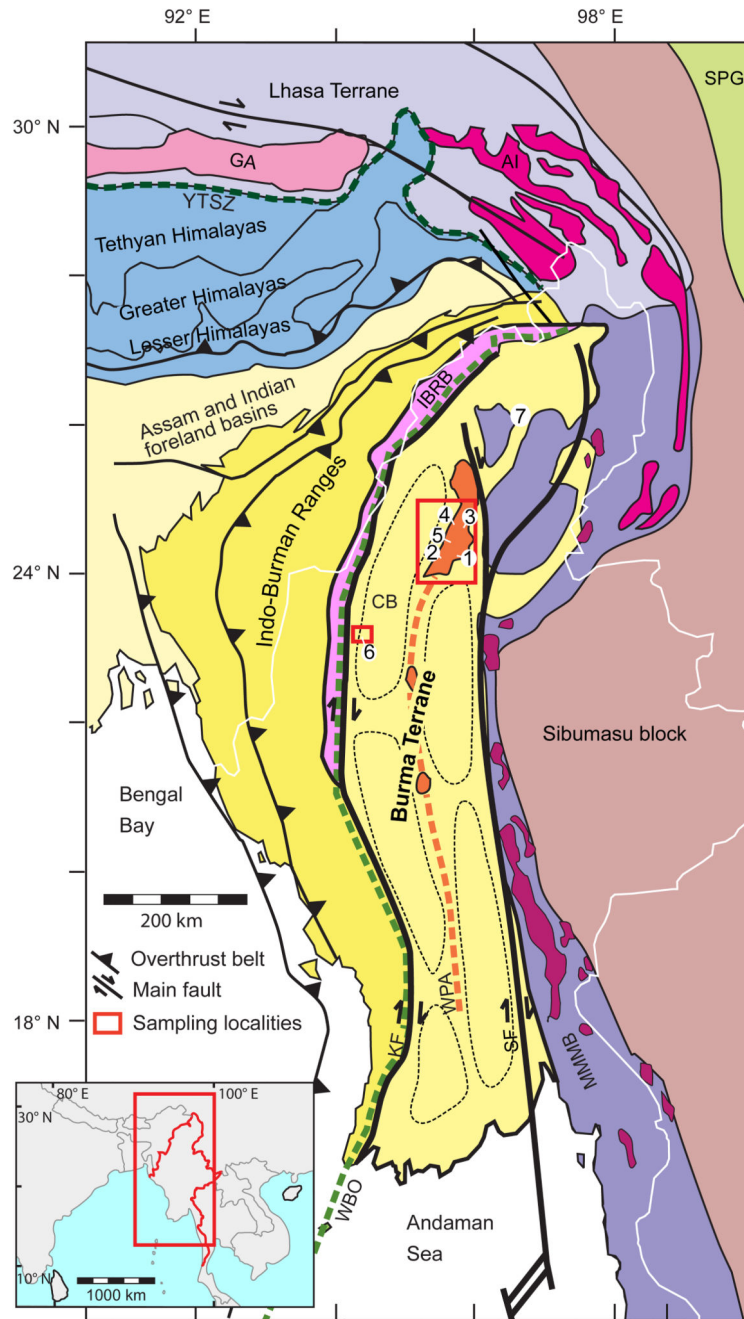


**Figure 2.** Generalized Myanmar geologic map<sup>21</sup>. Localities: 1 = Kawlin, 2 = Pinlebu, 3 = Banmauk, 4 = Kyaung Le, 5 = Shinpa, 6 = Kalewa, 7 = Burmese ambers<sup>18,19</sup>. Abbreviations: AI = Cretaceous-Paleogene Asian intrusives, CB = Chindwin Basin, GA = Cretaceous Gangdese Arc, IBRB: Indo-Burman Ranges basement, KF = Kabaw Fault, MMMB = Mogok–Mandalay–Mergui Belt (including Jurassic Eastern Belt Ophiolites & Jade Belt Ophiolite), SF = Sagaing Fault, SPG = Songpan Ganze & Yangtze complexes, WBO = Cretaceous

Western Belt Ophiolite, WPA = Wuntho-Popa Arc, YTSZ = Yarlung-Tsangpo Suture Zone.  
Dashed black lines: Central Myanmar Basins.

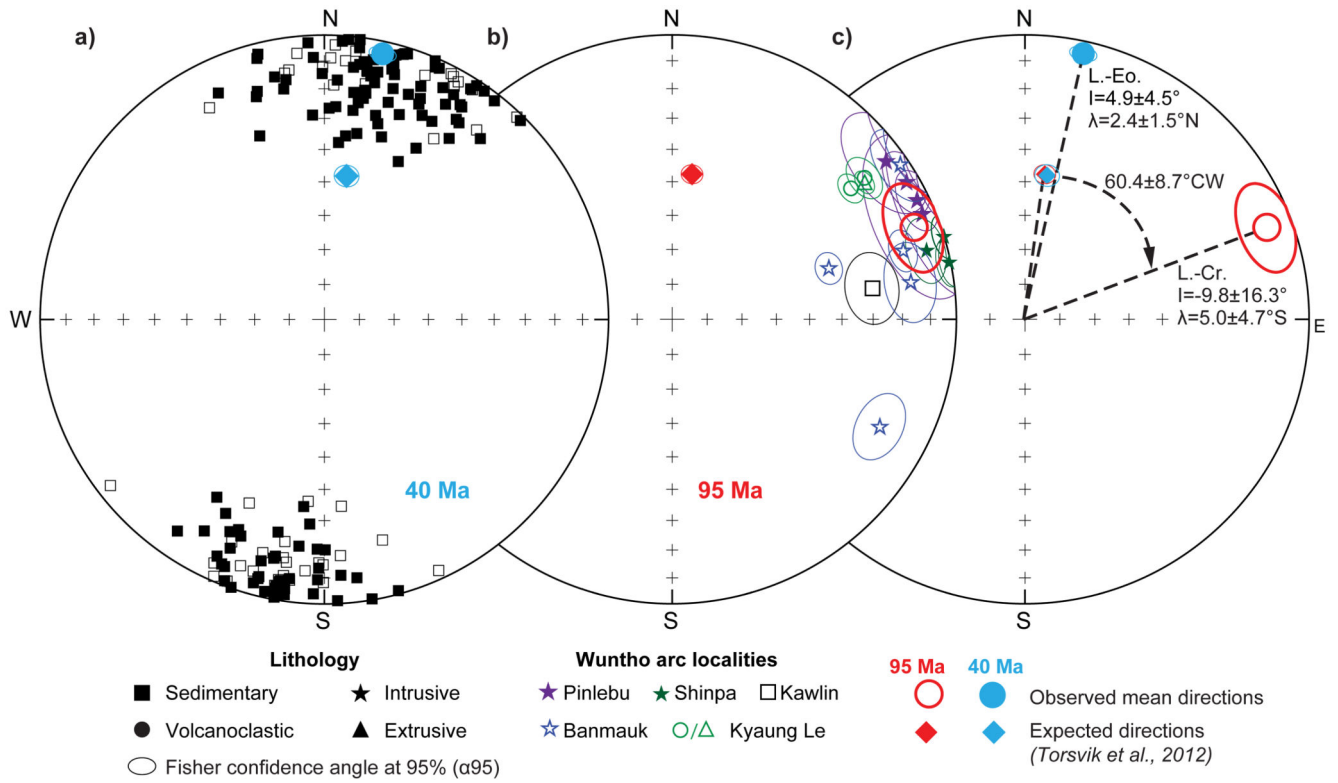


**Figure 3.** Equal-area projections of interpretable paleomagnetic results: a) Tilt-corrected characteristic directions (squares) of samples from upper Eocene sediments from Kalewa and mean direction (blue); b) Early Late Cretaceous Wuntho Range site means with 95% confidence angles in in-situ coordinates, coloured by locality: Pinlebu (purple), Shinpa (dark green), Banmauk (blue), Kawlin (black) and Kyaung Le (green) and mean direction (red); c) Early Late Cretaceous/late Eocene (red/blue circles) final mean directions compared with the stable Eurasia APWP in the early Late Cretaceous/late Eocene (red/blue diamonds) <sup>42</sup>. Corresponding paleolatitudes and rotation magnitudes are indicated with 95% confidence angles. Open/closed symbols denote negative/positive inclinations.

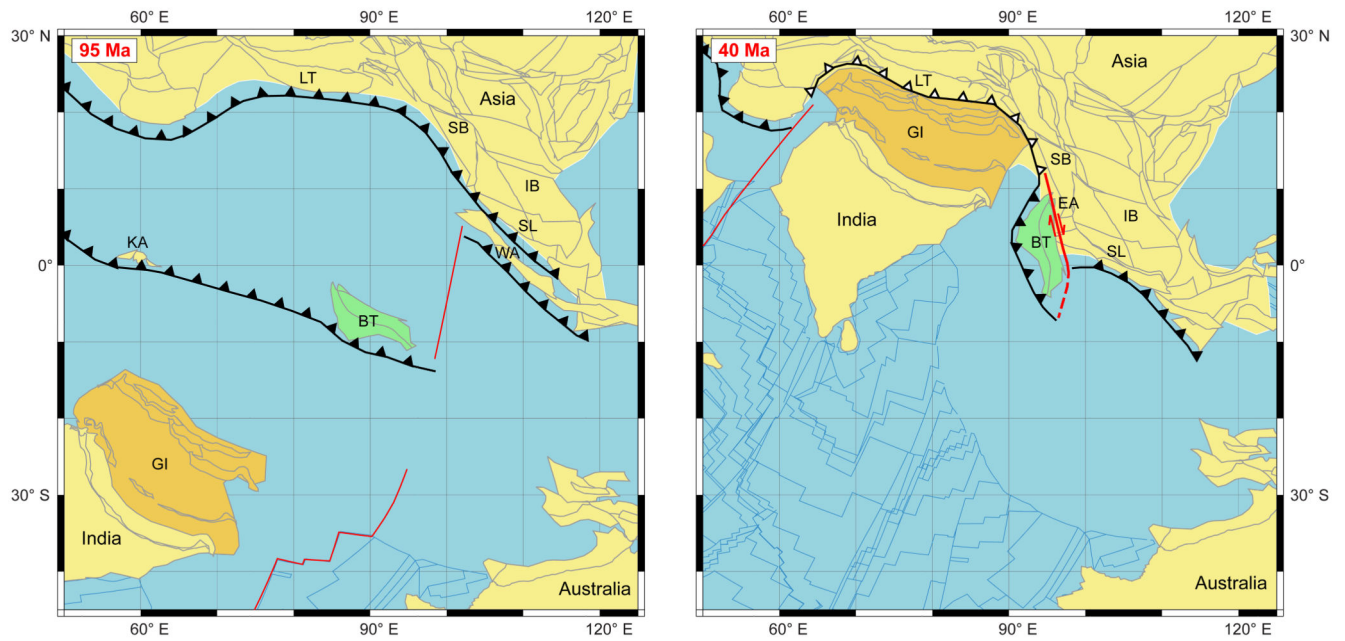


**Figure 4.** Reconstructions of the Burma Terrane and Asia at 95 Ma (left) and 40 Ma (right) with GPlates (See also Methods). Abbreviations: BT = Burma Terrane, EA = Eastern Andaman Basins, IB = Indochina Blocks, GI = Greater India, KA = Kohistan Arc, LT = Lhasa Terrane, SB = Sibumasu Block, SL = Sundaland, WA = Woyla Arc.